Structural basis for substrate discrimination and accommodation in bacterial site-2 protease homologue RseP

Intramembrane proteolysis is a unique cellular process wherein a polypeptide chain is hydrolyzed within the lipid bilayer [1]. Intramembrane proteolysis maintains the quality of the membrane by removing unnecessary and potentially cytotoxic membrane proteins. In addition, intramembrane proteolysis mediates signal transduction by cleaving the membrane-anchored precursor of signaling molecules such as transcription factors and secretory proteins. The deregulation of intramembrane proteolysis is also associated with human diseases such as cancer, Alzheimer's disease, and Parkinson's disease, while the signal transduction through the cleavage is implicated in pathogenic infections. Thus, how the substrates are cleaved within the lipid bilayer is an important biochemical and medical issue that must be addressed.

Intramembrane proteolysis is catalyzed by intramembrane proteases (IMPs) whose active center is within the transmembrane (TM) region. To date, four distinct families of IMPs (site-2 protease (S2P), presenilin/signal peptide peptidase, rhomboid, and Ras-converting enzyme1) have been identified across three domains of life [2]. Out of the four families, S2P was the first IMP to be isolated and classified as a zinc metalloprotease. As their names suggest, many of the S2P family members perform intramembrane proteolysis after the cleavage of their substrates in the soluble regions (site-1 cleavage). S2Ps activate transcription factors involved in the lipid metabolism and ER stress response in eukaryotes, while their prokaryotic homolog mediate signal transduction in extracytoplasmic stress responses and cell envelope biosynthesis. Each S2P cleaves several membrane proteins without apparent consensus on the primary structures. However, the cleavage is not promiscuous and its efficiency obviously varies depending on the substrate. Structural analysis is indispensable for understanding the molecular mechanism underlying the substrate discrimination by S2Ps, but the structural analysis of S2Ps had lagged behind that of other IMP families [3].

In this study, we performed crystallographic analysis on the *E. coli* S2P homolog RseP (*Ec*RseP) and its ortholog from the marine bacterium *Kangiella koreensis* (*Kk*RseP). *Ec*RseP was identified as an IMP to cleave a suppressor of the transcription factor and was further shown to remove remnant signal peptides from secretory proteins (Fig. 1). We purified *Ec*RseP using an immuno-affinity purification system termed the PAtag system to avoid denaturation. *Kk*RseP was discovered as the orthologue suitable for structural analysis. For phasing, we prepared selenomethionine (SeMet)-substituted *Kk*RseP. Diffraction-quality crystals were successfully obtained for both *Ec*RseP and SeMet-substituted *Kk*RseP in the lipidic cubic phase by adding an inhibitor batimastat. X-ray diffraction data were collected from microcrystals using the automated data collection system ZOO and processed by the KAMO system at SPring-8 **BL32XU**. Finally, we determined the crystal structures of *Ec*RseP and SeMet-substituted *Kk*RseP at 3.2 and 3.1 Å resolutions, respectively (Figs. 2(a,b)) [4].

Crystallographic analysis has revealed that the TM region of *Ec*RseP contains four membrane-spanning helices with a four-stranded membrane-reentrant β(MREβ)-sheet inserted between TM1 and TM2. The MREβ-sheet contains several charged residues on the cytoplasmic side and likely assists the recruitment of water molecules into the active center by excluding lipid molecules. The fourth strand of the MREβ-sheet is referred to as the edge strand and is located close to the active center. The peptide-mimetic inhibitor batimastat assumed an extended conformation and docked to the edge strand via hydrogen bonding between the main chains (Fig. 2(c)). Batimastat also forms hydrogen bonds with the side chain of Asn-394 on TM3. Structure-based mutational analysis suggested that the TM segment of the substrate should also be extended by the edge strand and clamped by Asn-394 for cleavage.

In addition, *Ec*RseP possesses two tandemly arranged PDZ domains (PDZ tandem) and the PDZ C-terminal (PCT) region between TM2 and TM3 on the periplasmic side. The PCT region contains two α-helices (PCT-H1 and H2) attached to the membrane surface and a loop connecting these two helices (PCT-loop). It has been proposed that the PDZ tandem suppresses the entry of bulky membrane protein into the active center [5]. PCT-H1 is also presumed to be involved in this size exclusion process. In fact, the PDZ tandem and PCT region lie just above the TM region and appear to restrict access to the active center. More specifically, PCT-H2 and PCT-loop surround the active center by interacting with TM4 via Asp-446 (Fig. 2(d)). The substitution of Asp-446 to residues other than glutamic acid substantially

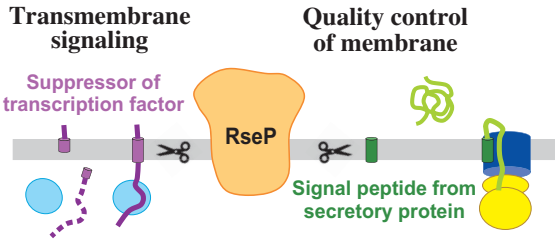

Fig. 1. Examples of the physiological roles of RseP in *E. coli*.

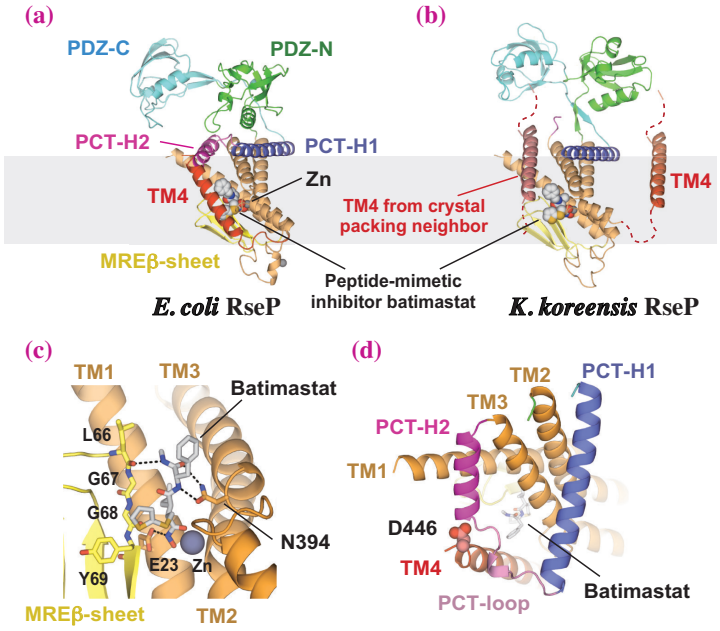

Fig. 2. Crystal structures of *Ec*RseP and *Kk*RseP. **(a)** *E. coli* RseP (*Ec*RseP). Polypeptide chains are shown as ribbon models. Batimastat and zinc ions (Zn) are shown as sphere models. **(b)** *K. koreensis* RseP orthologue (*Kk*RseP). The TM4 segment from the crystal packing neighbor is also shown in the ribbon diagram. **(c)** Close-up view of the batimastat binding site in *Ec*RseP. Batimastat, the residues forming hydrogen bonds with batimastat (Glu-23, Leu-66, Asn-394), and the three residues on the edge strand (Gly-67, Gly-68, Tyr-69) are shown as stick models. TM4 is omitted to visualize the binding site. **(d)** View of the *Ec*RseP model from an outside-in perspective relative to the membrane. The PDZ tandem is omitted to visualize the PCT region and TM domain. Asp-446 is shown as a sphere model.

reduces the substrate cleavage efficiency, indicating the importance of the electrostatic interaction between TM4 and the PCT region in the proteolytic reaction.

Furthermore, a structural comparison between *Ec*RseP and *Kk*RseP provided clues to help us understand the mechanism underlying the substrate accommodation. Despite the structural conservation of individual domains, *Kk*RseP showed marked conformational changes relative to *Ec*RseP (Figs. 2(a,b)). For instance, the PDZ tandem is positioned further away from the TM region, while the PCT-loop and PCT-H2 are unstructured. In *Kk*RseP, TM4 also moves away from the active center and docks to the cleft between TM1 and TM3 of the crystal packing neighbor, reminiscent of the binding mode with the substrates. These observations raised the possibility that the rearrangement of the domains surrounding the active center occurs during the substrate accommodation. In fact, we observed that intramolecular cross-links to fix the position of the PCT region reduced the proteolytic activity in *Ec*RseP.

From the results of our structural and biochemical analyses, we infer that the substrate discrimination and accommodation in *Ec*RseP are controlled by multiple processes, as summarized in Fig. 3. (1) Size exclusion process: The PDZ tandem suppresses the entry of bulky intact substrates by steric hindrance. After the cleavage of the periplasmic region (site-1 cleavage), the size-reduced substrates become accessible to the TM domain containing the active center. (2) Gating process: The PDZ tandem, PCT-H2, and TM4 undergo conformational changes to accommodate the substrate into the active center. Asp-446 may play a pivotal role in the cooperative movement of PCT-H2 and TM4. (3) Unwinding process: The edge strand of the MREβ-sheet extends the TM segment of the substrate and the side chain of Asn-394 clamps it for efficient cleavage. Our findings are expected to deepen our understanding of the mechanism underlying the substrate accommodation and cleavage in other IMPs including presenilin and rhomboid as they share common properties despite the difference in catalytic mechanism.

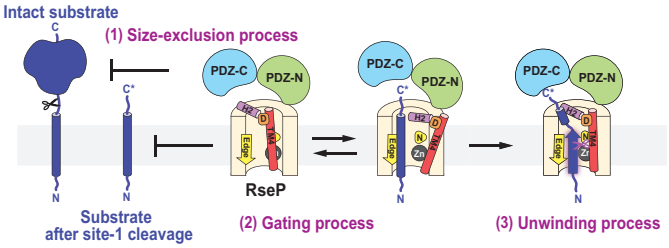

Fig. 3. Proposed model for substrate discrimination and accommodation in *Ec*RseP.

Yuki Imaizumi, Kazunori Takanuki and Terukazu Nogi*

Graduate School of Medical Life Science,
Yokohama City University

*Email: nogi@yokohama-cu.ac.jp

References

[1] M. S. Brown *et al.*: Cell **100** (2000) 391.
[2] N. Kühnle *et al.*: J. Cell Sci. **132** (2019) jcs217745.
[3] L. Sun *et al.*: Curr. Opin. Struct. Biol. **37** (2016) 97.
[4] *Y. Imaizumi, K. Takanuki, T. Miyake, M. Takemoto, K. Hirata, M. Hirose, R. Oi, T. Kobayashi, K. Miyoshi, R. Aruga, T. Yokoyama, S. Katagiri, H. Matsuura, K. Iwasaki, T. Kato, M. K. Kaneko, Y. Kato, M. Tajiri, S. Akashi, O. Nureki, Y. Hizukuri, Y. Akiyama, T. Nogi: Sci. Adv.* ***8*** *(2022) eabp9011.*
[5] Y. Hizukuri *et al.*: Structure **22** (2014) 326.